Optical Pump-Terahertz Probe Spectroscopy Utilizing a Cavity-Dumped Oscillator-Driven Terahertz Spectrometer

Bret N. Flanders, David C. Arnett, and Norbert F. Scherer

***Abstract*— A terahertz spectrometer capable of steady-state and time-resolved measurements over the 0.1–3.5-THz spectral region has been built. This spectrometer routinely produces and detects terahertz pulses that exhibit signal-to-noise ratios (SNR's) greater than 6000 in the time domain and a spectral noise floor of magnitude 2.7×10^{-4}. Hence, the spectrometer achieves nearly four decades of dynamic range in the frequency domain. Two pulse generation processes are observed to give rise to the measured terahertz pulse. High-quality optical pump-terahertz probe data on $\langle 111 \rangle$ GaAs samples are presented, demonstrating the applicability of this spectrometer to the study of optically induced dynamical processes. Non-Drude relaxation behavior is observed in the transient terahertz spectra.**

***Index Terms*—Cavity-dumped Ti:sapphire, optical pump-terahertz probe spectroscopy, time-resolved absorbance spectra.**

I. Introduction

GENERATION of pulsed terahertz radiation [1], [5] (1 THz = 33.3 cm^{-1} = 4.1 meV) that is useful for precise spectroscopic studies in the far-infrared (FIR) spectral region is crucial for obtaining experimental descriptions of condensed phase dynamical problems, such as reaction-induced solvent reorganization in liquid solutions. Such experimental information is relevant to understanding how reacting molecules lose excess energy and are, thereby, able to move out of the "transition state" to become "products" [2]–[4]. Part of this excess energy is due to orientational strain. This strain may be understood as a summation over the torques exerted by the solute electric field on the solvent molecules. This torque is strong immediately following the optically induced change in solute electronic state and, hence, dipole moment. As a result of this perturbation, the surrounding solvent molecules suddenly find themselves oriented at odds with respect to the excited solute electric field. The strain, then, is relaxed through reorientation of these molecules into more energetically (i.e., coulombically) favorable configurations. The degrees of freedom used in this equilibration process are translational and rotational motions that are resonant with and, therefore, absorb terahertz radiation. Hence, the process of reaction-induced molecular reorganization is, in principle, experimentally observable through the optical pump-terahertz probe measurement whereby the terahertz spectral response of the sample is measured at various times following the initiation of the reaction.

While numerous groups have successfully generated and measured terahertz pulses in the past 15 years [5], the spectroscopic applications, for the most part, have been steady-state measurements of the frequency dependent power absorption coefficient and index of refraction of semiconductors [6], molecular gases [7] and molecular liquids [8]–[11]. By contrast, the first optical pump-FIR probe experiment was performed a decade ago [12], and only a handful of such studies have since been reported [13]–[15]. Furthermore, the first *comprehensive* study of a reactive liquid solution still lies in the future. However, preliminary results on liquid solutions and molecular thin films have recently been reported [16]–[18].

Some requirements for construction of a spectrometer that is optimal for optical pump-probe studies may now be stated. Foremost in importance is the development of a terahertz pulse generation and detection system that is sensitive enough to detect the optical pump-induced response. Second, an intense optical pump source capable of initiating a large nonequilibrium response, in the sample, such as a chemical reaction, must be available. Finally, pulse-train repetition rates lower than the excited state decay rate of the solute molecule are necessary. One option for construction of a system characterized as stated is to employ the technique of cavity-dumping. The purpose of cavity-dumping a high-repetition-rate oscillator is to increase the pulse energy and provide control over the repetition-rate of the emitted pulse train. While amplification of high-repetition-rate oscillators is an obvious way to increase pulse energy, amplifiers introduce significant noise to the experimental system. Cavity-dumping is a good alternative if the desired increase in pulse energy (versus that of the mode-locked oscillator) is about one order of magnitude [19], [20]. The present home-built cavity-dumped Ti:sapphire (CD-TS) oscillator operates without additional noise (relative to the mode-locked output) in the cavity-dumped pulse train. A detailed description of the home-built oscillator system used herein is given elsewhere [20]. Cavity-dumped Ti:sapphire systems have recently been employed in numerous optical experiments in solutions [21]–[24]. A description of a cavity-dumped pulse-driven terahertz spectrometer whose performance satisfies the above requirements is the subject of this paper.

Manuscript received October 2, 1997; revised March 23, 1998.

B. N. Flanders and N. F. Scherer are with the Department of Chemistry and the James Franck Institute, University of Chicago, Chicago, IL 60637 USA.

D. C. Arnett is with the Department of Chemistry, University of Pennsylvania, Philadelphia, PA 19104-6323 USA.

Publisher Item Identifier S 1077-260X(98)04191-4.

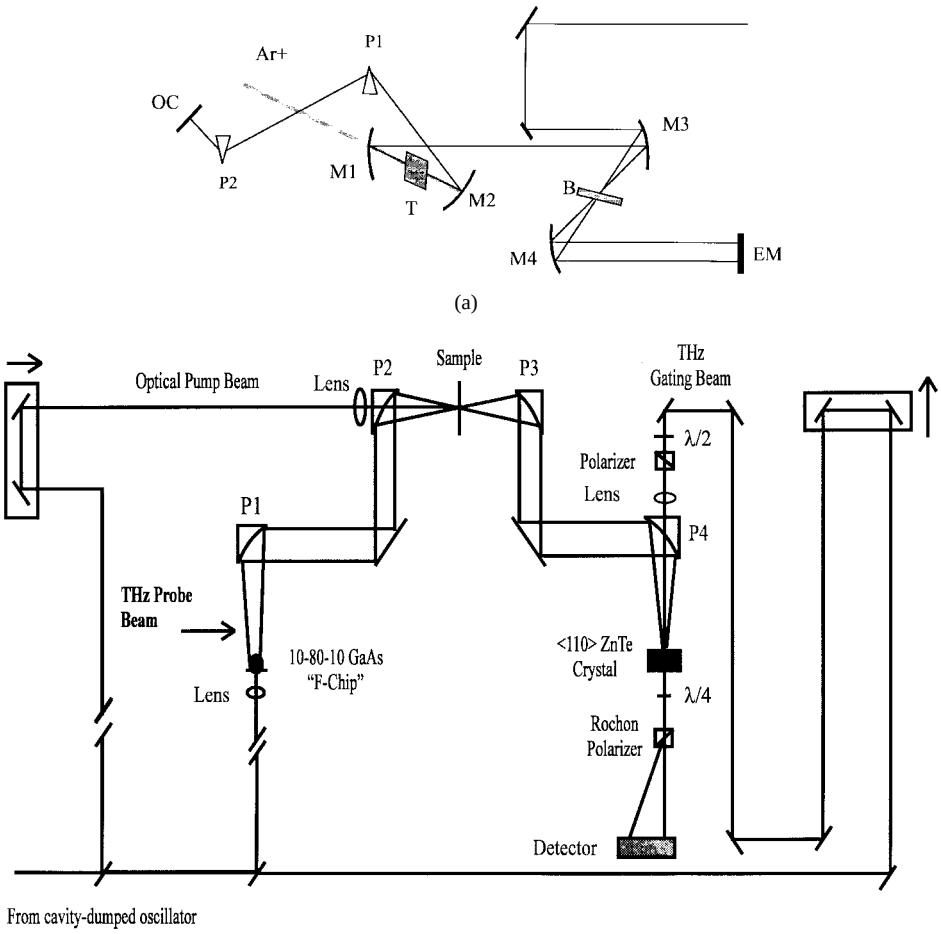

Fig. 1. (a) A diagram of the cavity-dumped Ti:sapphire oscillator. The black line indicates the optical path and the gray line indicates the Ar^+ pump beam. OC refers to the 2% output coupler, P1 and P2 to intracavity fused silica prisms, M1 and M2 to 10 cm radius of curvature focusing mirrors, M3 and M4 to 15 cm radius of curvature focusing mirrors, T to the Ti:sapphire crystal, B to the Bragg cell and EM to the high-reflecting end mirror. (b) A diagram of the optical pump-terahertz probe spectrometer is presented. The single black line indicates the path taken by optical beams and the double black lines marks the path followed by the terahertz beam. P1–1P4 refer to paraboloidal reflectors

The paper is organized as follows. A detailed description of the experimental apparatus is provided in Section II including characterization of the terahertz pulses. Section III discusses the novel, hybrid approach employed for generation of terahertz radiation via cavity-dumped pulse excitation of the terahertz source. Use of the optical pump-terahertz probe spectrometer for the study of carrier dynamics in $\langle 111 \rangle$ GaAs is then discussed in Section IV. General conclusions are made in Section V.

II. Experimental

The home-built cavity-dumped oscillator shown in Fig. 1(a) is based on the "standard" four-mirror Kerr-lens mode-locked Ti:sapphire oscillator [25]–[27], and is capable of generating sub-20-fs pulses. Two 15-cm radius of curvature mirrors were added in a Z-fold configuration surrounding a 3-mm-wide fused-silica Bragg cell; the latter is situated at the focal point between these two mirrors and is oriented so that the lasing radiation is Brewster incident upon the faces of the cell. The delay (distance) between the Bragg cell (B) and the end mirror (EM) is adjusted corresponding to the design of Arnett *et al.* [20]. That is, the distance is set so that temporal coincidence in the Bragg cell between the outward-going optical pulse and the maximum of one oscillation of the RF pulse and between the returning pulse and the next maximum of the RF pulse (delayed by 2.5 ns) is obtained. This improved timing with the RF pulse maxima allows dumping $>$80% of the intracavity energy, although 60%–70% dumping is chosen for improved long term stability. Pulse-to-pulse intensity fluctuations are the same as a four-mirror oscillator, and long term stability is only slightly degraded. Pre-/postpulse contrast is $>$500:1 and residual pulse chirp is compensated with extra-cavity fused silicon prisms.

The output of the CD-TS laser, characterized by a 250-kHz pulse train delivering 15-mW average power in 60-nJ pulses, is directed into the optical pump-terahertz probe spectrometer illustrated in Fig. 1(b) In this experimental configuration, a 50/50 pellicle beam splitter (3 μm thickness) is used to direct a portion of the main beam [termed optical pump beam in Fig. 1(b)] onto the first time delay stage for the purpose of introducing an optical perturbation in the sample. This stage delays the arrival of the optical pump pulse relative to the arrival time of the peak of the terahertz probe pulse. The

optical power in this pump beam is typically 4.0 mW and, thereby, delivers a 16-nJ pulse to the sample. A $f = 6.25$-cm doublet lens is used to focus the pump beam through a 2.0-mm hole along the optical axis of the Au-coated paraboloid into the sample. Corrections in the position of the pump beam on the sample may be made through small translations of this lens.

The transmitting antenna structure, described in detail elsewhere [28], [29], is composed of two 10-μm-wide gold transmission lines on a semi-insulating GaAs wafer. The separation between the parallel lines is 80 μm and a +65-V bias is applied to the transmitter. The 0.8 mW of 790-nm Ti:sapphire radiation is focused with a $f = 2.5$-cm diode doublet lens onto the "F-chip" source producing a sudden population of carriers in the region of the GaAs between the two transmission lines. The GaAs is irradiated with a defocused optical beam (diameter ~ 50 μm) to prevent premature circuit burnout by the potentially excessive current in the antenna generated by the more intense, sharply focused cavity-dumped pulse. The approximately half-toroidal volume of terahertz radiation emitted from the back side of the GaAs wafer is collected by a high-resistivity Si lens. A paraboloidal-flat-paraboloidal combination of Au-coated mirrors is used to collimate, direct and focus the beam of terahertz pulses into the sample, respectively. A similar combination of optics is used to collect, direct and focus the terahertz beam into a 1.5-mm-thick $\langle 110 \rangle$ ZnTe electrooptic sensor, where the terahertz signal is detected by the Pockel's effect [30].

III. Results and Discussion

A. Dynamic Range of Spectrometer

Fig. 2(a) illustrates the measured terahertz electric field profile (in bold) obtained without a sample present. This trace is an average of 6–7-ps duration, 280 data point scans, each requiring four minutes of data acquisition time. The noise associated with this temporal profile is shown at negative delay time (light solid line), and is magnified by a factor of 1000. The optical gating beam passes through the ZnTe EO sensor, a $\lambda/4$ plate and a Rochon beam-splitting polarizer and is incident on a pair of balanced photodiodes (New Focus "Nirvana"). The signal-to-noise ratio (SNR) of the resulting averaged pulse is 6300. This value was obtained through calculation of the standard-of-deviation of the noise (shown in expansion) followed by inversion and multiplication by the peak signal value (which in this case was unity). An alternative method for the determination of this quantity is explained below.

Fig. 2(b) illustrates the spectral characteristics of the measured terahertz pulse. This spectrum results from Fourier-transformation of the measured temporal profile. The lighter trace in Fig. 2(b) represents the noise spectrum of the detection system in the terahertz spectrometer. For this measurement, the bias across the antenna was removed and the optical beam incident on the terahertz source was blocked in order to eliminate any contaminating terahertz field generated via rectification [31]. Only the probe beam still illuminated the detection optics and photodiodes. An average of 6-7-ps scans was acquired, as in the previous measurement of the terahertz pulse, and was Fourier transformed to give the noise spectrum.

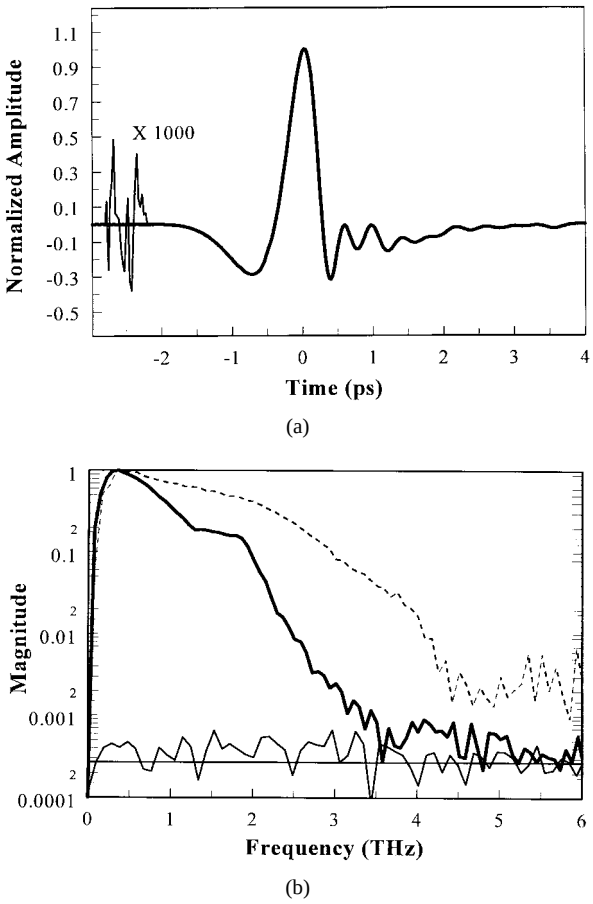

Fig. 2. (a) The temporal profile of the terahertz pulse is presented. The magnified portion illustrates the noise level on the measured terahertz signal. (b) The spectrum of the CD-THz pulse detected by a ZnTe electrooptic sensor is denoted by a bold line. The dashed line represents the OC-THz signal detected by a gated antenna. The noise floor of the terahertz spectrometer is indicated by the light solid line as well as the average in the thin horizontal line with a value of 2.7×10^{-4}.

As evident in this figure, the noise floor for this terahertz spectrometer was found to lie at 2.7×10^{-4} allowing nearly four decades of dynamic range. The inverse of this number is roughly 3700, yielding a second (relative to the value of 6300 reported above) value for the SNR. This technique of reporting SNR probably yields the more legitimate result because it clearly reflects the limiting spectral magnitude for signal detectability. Fig. 2(b) also indicates that the bandwidth of the terahertz pulse extends to above 3.5 THz. For comparison with the pulse spectrum measured by this low-repetition-rate, cavity-dumped terahertz (CD-THz) spectrometer, the spectrum obtained from a 84 MHz, output-coupled terahertz (OC-THz) spectrometer [8] (employing an antenna-type of detector) is illustrated as the dashed line in Fig. 2(b). The OC-THz spectrum is somewhat broader than the CD-THz result. However, the CD-THz spectrum demonstrates dynamic range greater than that of the high-repetition-rate system; the roughly constant signal level of the OC-THz spectrum above 5.0 THz indicates a value of about 3.0×10^{-3} for the associated noise floor. Thus, the measured dynamic range of the CD-THz signal is roughly an order of magnitude greater at frequencies below 2 THz.

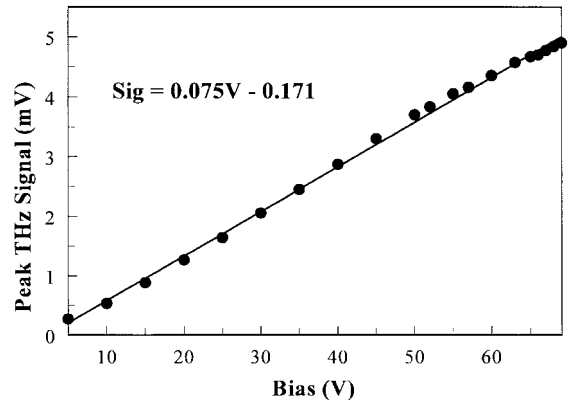

(a)

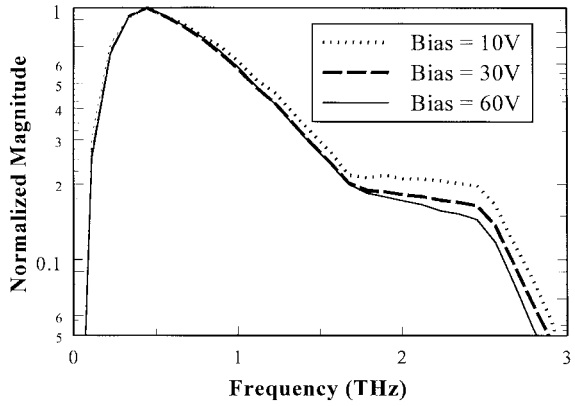

(b)

Fig. 3. (a) The terahertz peak signal dependence on applied dc-bias is represented by the solid points. The solid line is a linear fit to the data. (b) The normalized spectral magnitudes are indicated for applied bias values of 10 V (dotted), 30 V (heavy dash) and 60 V (solid line).

B. Mechanism for Terahertz Generation

The difference in appearance between the spectral profiles of the CD-THz and OC-THz signals in Fig. 2(b) is indicative of a difference between the mechanisms of terahertz pulse generation and detection. Sensitivity to the pulse generation mechanism is further borne out in a comparison of the (temporal) peak terahertz signal dependence on applied dc bias. The peak value of the terahertz signal was observed to scale linearly with applied bias from 0 to +70 V illustrated in Fig. 3(a). Conversely, the peak OC-THz signal's voltage dependence was observed to be nonlinear when optical illumination of the source is near the anode, especially at higher values of applied bias where the dependence exhibits obvious cubic behavior [28], [29]. This linear dependence is reminiscent of the bias dependence of the peak terahertz amplitude that is generated from 30-μm-long antenna structures on SOS substrates. In this case, a linear signal-bias dependence was observed and the carrier dynamics in the source antenna were attributed to ohmic conduction [32].

Fig. 3(b) presents the bias dependence of the terahertz signals presented in a way that is more sensitive to the deviations from the (observed) linear peak terahertz signal dependence. Fig. 3(b) illustrates the frequency-domain magnitude spectra of a series of terahertz pulses measured with different dc voltages applied to the source antenna. These spectra were plotted in semilog format and normalized to the peak at 0.5 THz. Because the spectra are normalized, the different linear amplification factors for the different dc-bias values are eliminated. Hence, the nonoverlapping spectral line shapes indicate that a nonlinear terahertz generation process contributes to the observed terahertz signal. The mechanism for nonlinear (with respect to applied bias) generation of the terahertz pulse is likely to be the same mechanism responsible for OC-THz generation given the identical structure of the terahertz sources. This process was originally attributed by Grischkowsky and co-workers [28], [29] in their characterization of the GaAs F-chip source to hole injection at the anode due to high localized fields in the anode region of the chip. That is, it is known [24] that defects in GaAs have a larger capture cross section for electrons than for holes. Therefore, on illumination of the antenna in the 5-μm region near the anode (+65 V), the holes are accelerated toward the cathode (0 V) whereas the electrons (or a subset thereof) become trapped near the anode. Hence an increased electron density exists in a micron-sized illuminated area near the anode. This effectively static body of charge gives rise to an enhanced local field that lowers the barrier to hole injection from the anode. This second source of electrical carriers gives rise to a net nonlinear current, and, consequently, a nonlinear terahertz signal dependence on applied bias. Indeed, a nonlinear peak signal dependence on dc-bias was observed in the OC-THz generation study [29]; however, a linear dependence is observed in the CD-THz case. The explanation for this inconsistency is that the nonlinear signal effect is present in the CD-THz signal, but is not easily observable in the apparently linear peak terahertz-voltage data. That is, CD-THz generation involves a diminished nonlinear contribution relative to the magnitude of the nonlinear contribution in OC-THz generation.

Further support for this view regarding the reduced yet finite magnitude of the nonlinear mechanism in CD-THz generation may be obtained from a carrier population-based analysis of the two terahertz generation techniques. The approximate calculation of the carrier density is useful for performing this population analysis. This quantity may be defined as $\rho_C = N_C/V_P$ where ρ_C is the carrier density, V_P is the volume occupied by the carriers which absorb the optical radiation and N_C is the number of optically created carriers per pulse. V_P was approximated by a cylindrical volume of height equal to an optical penetration depth of 700 nm [33] and radius equal to the focused beam radius. The calculation of N_C took into account the reflectivity ofr GaAs of 33% [33]. For a 0.8-mW pulse train with a repetition rate of 250 kHz, the number of carriers is determined to be $N_C^{\mathrm{CD}} = 1.6 \times 10^{10}$ per pulse and the carrier density per pulse[1] corresponding to a 50-μm spot diameter is calculated to be $\rho_C^{\mathrm{CD}} = 1.2 \times 10^{19}$ carriers/cm^3. For the OC-THz generation technique, the 84-MHz 2.5-mW optical beam is focused to a 5-μm beam diameter on the terahertz source, so the number of carriers created per optical pulse is calculated to be $N_C^{\mathrm{OC}} = 1.5 \times 10^8$. Hence, the carrier density per pulse corresponding to a 5-μm spot diameter

[1] It is assumed that a quantum yield of one is realistic for photon-to-electron conversion.

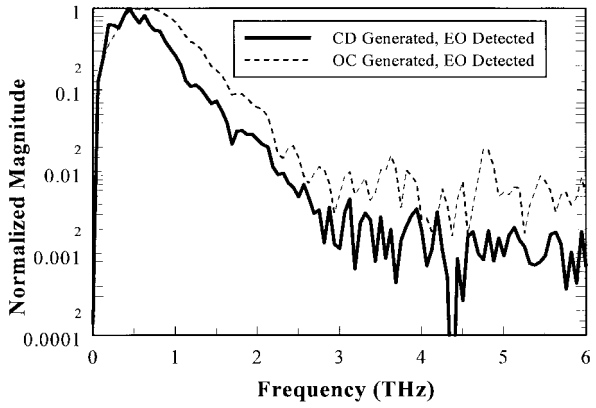

Fig. 4. The magnitude spectrum of a measured CD-THz pulse measured electrooptically is shown as the solid line. The magnitude spectrum of a previously measured OC-THz pulse measured electrooptically is indicated by the dashed line.

for the OC-THz generation technique is $\rho_C^{\mathrm{OC}} = 1.1 \times 10^{19}$ carriers/cm^3. Therefore, the carrier densities for the CD- and OC-THz generation techniques are roughly equal. However, the carriers in the CD-THz case are distributed over a much larger region. The quantity $P^{\mathrm{NL}} = (V_P^{\mathrm{OC}} \rho_C^{\mathrm{CD}})/N_C^{\mathrm{CD}}$ yields the percentage of CD-THz generated carriers that are created in the 5-μm region near the anode, where the increased electron density must exist in order for the enhanced field effect to be large enough to induce hole injection. Only 1% of the total number of carriers created per cavity-dumped pulse are nascent inside of this 5-μm region. Therefore, hole injection [28] and the resulting nonlinear conduction of the carriers, an effect that is not possible in low-field regions far from the anode, are attributed to motion by this (small) fraction of electrical carriers. The remaining carriers are created outside of the anode region and are, therefore, linearly conducted across the antenna. The dc-bias dependence of the peak terahertz signal is dominated by these ohmically conducted carriers. Hence, the observed peak terahertz signal dependence on applied bias appears linear. The combination of these two observations, the linear peak terahertz-voltage dependence and the nonlinearity apparent in the terahertz magnitude-voltage dependence, indicate that (at least) two terahertz generation mechanisms give rise to the terahertz pulse generated by the cavity-dumped oscillator-powered terahertz spectrometer.

Another effect, optical rectification [31] of the source, might contribute to the nonlinear bias dependence indicated by the differences in the spectra of Fig. 3(b). This second source of terahertz radiation would cause the dc voltage dependence of the signal amplitude to appear to behave in a nonlinear fashion, especially at lower bias values, since rectification is independent of bias. However, this effect is not apparent in the voltage dependence shown in Fig 3(a). Moreover, when the applied bias was removed, no terahertz signal polarized along the axes to which the detection optics are sensitive was observed.

It should be noted that another difference between the OC-THz and CD-THz spectra of Fig. 2(b) lies in the detection schemes employed for each of the measurements (EO sensor versus photo-conductive receiver). The measurements illustrated in Fig. 4 employ EO detection with both a CD-THz and an OC-THz source configuration. The spectral profile of the OC-THz spectrum, though smaller in magnitude, is similar to the CD-THz spectrum. Hence, the photo-conductive receiver (10-μm–20-μm–10-μm SOS type antenna) used for the OC-THz signals of Fig. 2(b), where greater high frequency magnitude is observed, may have a spectral response that is skewed toward higher frequencies than the EO scheme. This effect may partially explain the broader bandwidth of the OC-THz magnitude spectrum in Fig. 2(b).

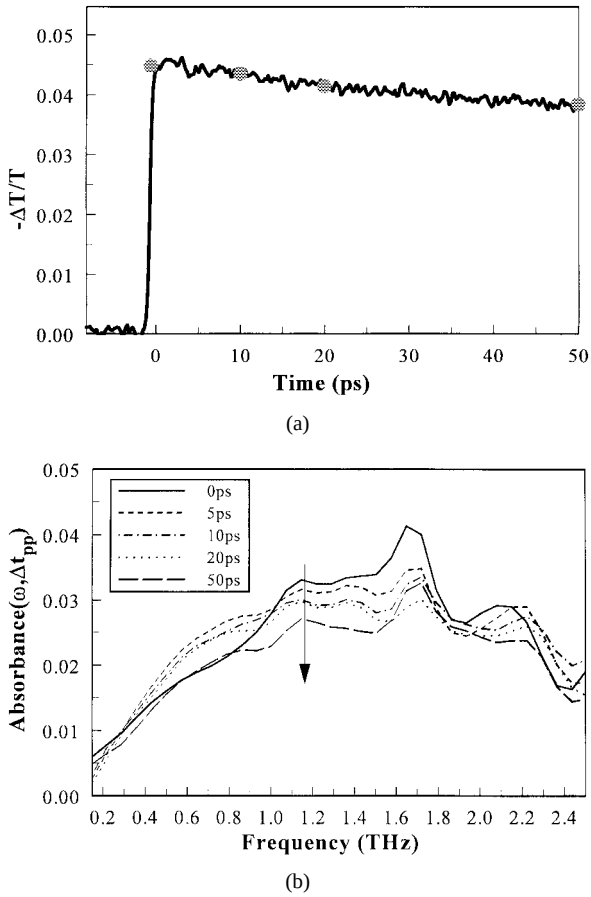

Fig. 5. (a) The minus differential transmission optical pump-terahertz probe data of $\langle 111 \rangle$ GaAs is represented by the solid black line. The gray points represent the time delays (0, 10, 20, and 50 ps) at which the transient absorbance measurements were performed. (b) The transient absorbance profiles are shown for pump-probe time delays of 0, 10, 20, and 50 ps.

C. Application: Pump-Probe Data of $\langle 111 \rangle$ GaAs

Optical pump-terahertz probe data obtained with this spectrometer is illustrated in Fig. 5(a), where the transient terahertz transmission for a 450-μm-thick wafer of undoped $\langle 111 \rangle$ GaAs is recorded as a function of time following optical pump pulse excitation. The data are recorded with the optical gating beam at the maximum amplitude of the terahertz pulse; the time axis refers to the pump-probe delay time obtained by scanning the optical beam delay stage [see Fig. 1(b)]. Reduced transmission of the probe beam occurs due to the pump-induced sample absorbance of terahertz frequencies by the photogenerated carriers. An upper limit for the photoexcited carrier density corresponding to a 16 nJ pulse, a focused beam

diameter of 1 mm, a reflectivity for GaAs of 33%, and an optical penetration depth of 700 nm [33][1] is estimated to be 1.5×10^{17} carriers/cm. This signal was detected in a double beam modulation scheme, in which both the pump beam and the terahertz source excitation beam were chopped. This step is necessary because rectification of the optical pump by the $\langle 111 \rangle$ GaAs sample causes a contaminating second terahertz pulse to be incident on the receiver. This step, however, reduces the signal level by roughly a factor of three, so the SNR is considerably reduced. Fig. 4(a) also indicates the 4.5% modulation depth of the optically induced response. Although the level of this pump-induced change is modest [34],[2] the SNR of 83 demonstrates the excellent sensitivity of this apparatus.

Fig. 5(b) illustrates the time dependent absorbance spectra attained at various pump-probe delay times. These data are referenced to the steady-state absorbance spectrum for the measured GaAs sample. The plotted function is

$$\mathrm{abs}(\omega, \tau) \equiv -2 \ln \left[\frac{|E_{\mathrm{ref}}(\omega) - E_{\mathrm{sig}}(\omega)|}{|E_{\mathrm{ref}}(\omega)|} \right]$$

where $|E_{\mathrm{ref}}(\omega)|$ and $|E_{\mathrm{sig}}(\omega)|$ are the magnitude spectra for steady-state and optically induced terahertz transmission through the GaAs sample, respectively. This function yields the expected decreasing time-resolved absorbance signal with decreasing strength of $E_{\mathrm{sig}}(\omega)$. Therefore, the spectra should be zero when pump-initiated events do not give rise to absorption and the probe frequencies that are absorbed are just those of the steady-state spectrum. Hence, the series of spectra in Fig. 5(b) are termed time-resolved absorbance spectra. It is noted that the structure around 1.7 THz is due to truncation effects that result from numerical Fourier transformation of the finite length temporal data.

These data deviate substantially from the Drude model analysis performed on GaAs $\langle 100 \rangle$ at higher pump excitation energies [12], [35]. In particular, in the spectral region between 0.2 and 1.0 THz, the magnitude of the pump-initiated absorption response at $\tau = 0$ lies below the spectra corresponding to $\tau \geq 5$ ps. This growth over time indicates that processes other than carrier relaxation, for which the opposite trend is expected, are occurring on the time scales of less than 5 ps. Consideration of the spectrally broad, above-bandgap optical pulse used to excite electron population into the conduction band clarifies this deviation. Other studies on semiconductors have determined that carriers rapidly scatter on time scales less than 300 fs [36] out of the high mobility, highly absorbing lowest lying Γ valleys into higher lying valleys (L and X) where absorption of FIR radiation occurs to a lesser extent [12], [35], [36]. The back scattering process $L \rightarrow \Gamma$ was found to occur on an approximately 2-ps time scale [12], [35]. This time scale is consistent with the low frequency growth in absorption illustrated in Fig. 5(b). A major difference between the current and earlier studies is that the optical excitation wavelength, centered here at 790 nm, is less energetic. Hence, a smaller population of initially excited carriers is expected to be able to access these other valleys. Indeed, such dynamics are not even evident in the time domain data in Fig. 5(a), in contrast to the frequency integrated time domain data obtained with 580–700-nm optical excitation [35]. However, in the more sensitive, spectrally resolved presentation of the pump-probe data in Fig. 5(b), increased absorption is observed. It is logical to infer, therefore, that a smaller proportion of carriers reaches the higher valleys due to the lower excitation wavelength. It was determined that around 60% of the pump-created carriers access the higher valleys when excited with a pulse centered around a wavelength of 700 nm [35]. In the present case, this proportion of carriers is, of course, less even considering the 50-nm bandwidth of the pump-pulse. However, the ability to attain spectrally resolved data makes these rather weakly induced dynamics observable and thereby testifies to the sensitivity of the current instrument.

The spectral range between 1–1.8 THz illustrates monotonically decreasing absorption strength with increasing pump-probe delay time, as indicated by the downward pointing arrow. This dependence is most likely due to cooling of optically generated electron population in the conduction band. However, since the exciton binding energy in GaAs is about 1 THz [37], spectral contributions form exciton formation and relaxation dynamics may be present in the data. Pump wavelength dependent and temperature dependent studies will be employed to extract the different contributions to the transient terahertz spectra. Further measurements of this and other semiconductor and organic crystal systems are in progress.

[2] 80% modulation depth from GaAs has been observed using amplified optical pump studies in a single-beam modulation configuration.

IV. Conclusion

An innovative optical pump-terahertz probe spectrometer has been constructed and described in detail. The terahertz pulses that are routinely detected demonstrate nearly four decades of spectral dynamic range and a bandwidth extending to above 3.5 THz. The dynamic range is shown to be nearly an order of magnitude greater than that obtained with a comparable high repetition rate spectrometer. Finally, high-quality pump-probe data on GaAs demonstrates the applicability of this spectrometer to the study of complex relaxation processes in condensed phase media. Investigations of conducting polymers and charge-transfer reactions in solution are underway.

References

[1] D. H. Auston, "Sub-picosecond electro-optic shock waves," *Appl. Phys. Lett.*, vol. 43, pp. 713–715, 1983.
[2] M. Cho, Y. Hu, S. J. Rosenthal, D. C. Todd, M. Du, and G. R. Fleming, "Friction effects and barrier crossing," in *Activated Barrier Crossing*, G. R. Fleming and P. Hanggi, Eds. River Edge, NJ: World Scientific, 1993, pp. 143–162.
[3] D. Raferty, R. J. Sension, and R. M. Hochstrasser, "Chemical aspects of solution phase reaction dynamics," in *Activated Barrier Crossing*, G. R. Fleming and P. Hanggi, Eds. River Edge, NJ: World Scientific, 1993, pp. 163–205.
[4] J. Schroeder and J. Troe, "Solvent effects in the dynamics of dissociation, recombination and isomerization reactions," in *Activated Barrier Crossing*, G. R. Fleming and P. Hanggi, Eds. River Edge, NJ: World Scientific, 1993, pp. 206–240.
[5] D. H. Auston, in *Picosecond Optoelectronic Devices*, C. H. Lee, Ed. London, U.K.: Academic, pp. 73–116, 1984.
[6] T.-I. Jeon and D. Grischkowsky, "Nature of conduction in doped silicon," *Phys. Rev. Lett.*, vol. 78, pp. 1106–1109, 1997.

[7] R. A. Cheville, H. Harde, and D. Grischkowsky, "Terahertz studies of collision-broadened rotational lines," *J. Phys. Chem. A*, vol. 101, pp. 3646–3660, 1997.
[8] B. N. Flanders, R. A. Cheville, D. Grischkowsky, and N. F. Scherer, "Pulsed terahertz transmission spectroscopy of liquid $CHCl_3$, CCl_4 and their mixtures," *J. Phys. Chem.*, vol. 100, pp. 11824–11835, 1996.
[9] B. N. Flanders, P. Moore, R. A. Cheville, M. L. Klein, D. Grischkowsky, and N. F. Scherer, "Pulsed terahertz study and spectral analysis of a simple solution: HCl in CCl_4," in *Tech. Dig. QELS'97*, May 1997, pp. 115–116.
[10] L. Thrane, R. H. Jacobsen, Uhd Jepsen, and S. R. Keiding, "THz reflection spectroscopy of liquid water," *Chem. Phys. Lett.*, vol. 240, pp. 330–333, 1995.
[11] J. T. Kindt and C. A. Schmuttenmaer, "Far-infrared dielectric properties of polar liquids probed by femtosecond terahertz pulse spectroscopy," *J. Phys. Chem.*, vol. 100, pp. 10373–10379, 1996.
[12] M. C. Nuss, D. H. Auston, and F. Capasso, "Direct sub-picosecond measurement of carrier mobility of photo-excited electrons in gallium-arsenide," *Phys. Rev. Lett.*, vol. 58, pp. 2355–2358, 1987.
[13] B. I. Greene, P. N. Saeta, D. R. Dykaar, S. Schmitt-Rink, and S. L. Chuang, "Far-infrared light generation at semiconductor surfaces and its spectroscopic applications," *IEEE J. Quantum Electron.*, vol. 28, pp. 2302–2312, 1992.
[14] R. M. H. Groenveld and D. Grischkowsky, "Picosecond time-resolved far-infrared experiments on carriers and excitons in GaAs-AlGaAs multiple quantum wells," *J. Opt. Soc. Amer. B*, vol. 11, pp. 2502–2507, 1994.
[15] B. B. Hu, E. A. Souza, W. H. Knox, J. E. Cunningham, M. C. Nuss, A. V. Kuznetsov, and S. L. Chuang, "Identifying the distinct phases of carrier transport in semiconductors with 10fs resolution," *Phys. Rev. Lett.*, vol. 74, pp. 1689–1692, 1995 .
[16] R. McElroy and K. Wynne, "Pump-probe spectroscopy in the condensed phase with THz pulses, "in *Tech. Dig. QELS'97*, May 1997, p. 83.
[17] ———, "Ultrafast dipole solvation measured in the far-infrared," *Phys. Rev. Lett.*, vol. 79, pp. 3078–3081, 1997.
[18] G. Haran and R. M. Hochstrasser, "Femtosecond far-infrared pump-probe spectroscopy: A new tool for studying low frequency vibrational dynamics in condensed phases," *Chem. Phys. Lett.*, vol. 274, pp. 365–371, 1997.
[19] M. S. Pshenichnikov, W. P. de Boeij, and D. A. Wiersma, "Generation of 13fs, 5MW pulses from a cavity-dumped Ti:sapphire laser," *Opt. Lett.*, vol. 19, pp. 572–574, 1994.
[20] D. C. Arnett, M. A. Horn, and N. F. Scherer, to be submitted.
[21] D. C. Arnett, P. Vöhringer, and N. F. Scherer, "Excitation dephasing, product formation and vibrational coherence in an intervalence charge transfer reaction," *J. Amer. Chem. Soc.*, vol. 117, pp. 12262–12272, 1995.
[22] D. M. Jonas, M. I. Lang, Y. Nagasawa, T. Joo, and G. R. Fleming, "Pump-probe polarization anisotropy study of femtosecond energy transfer within the photosynthetic reaction center of Rhodobacter Sphaeroides R26," *J. Phys. Chem.*, vol. 100, pp. 12660–12673, 1996.
[23] M. S. Pshenichnikov, K. Duppen, and D. A Wiersma, "Time-resolved femtosecond photon echo probes bimodal solvent dynamics," *Phys. Rev. Lett.*, vol. 74, pp. 674–677, 1995.
[24] M. J. Feldstein, C. D. Keating, Y. H. Liau, M. J. Natan, and N. F. Scherer, "Electronic relaxation dynamics in coupled metal nanoparticles," *J. Amer. Chem. Soc.*, vol. 119, pp. 6638–6647, 1997.
[25] F. Krausz, Ch. Spielmann, T. Brabec, E. Wintner, and A. J. Schmidt, "Generation of 33fs optical pulses from a solid state laser," *Opt. Lett.*, vol. 17, pp. 204–206, 1992.
[26] M. T. Asaki, C. P. Huang, D. Garvey, J. Zhou, H. C. Kapteyn, and M. M. Murnane, "Generation of 11fs pulses from a self-mode-locked Ti:sapphire laser," *Opt. Lett.*, vol. 18, pp. 977–979, 1993.
[27] P. Vöhringer, R. A. Westervelt, T. S. Yang, D. C. Arnett, M. J. Feldstein, and N. F. Scherer, "Solvent and frequency dependence of vibrational dephasing on femtosecond time-scales," *J. Raman Spec.*, vol 26, pp. 535–551, 1995.
[28] N. Katzenellenbogen and D. Grischkowsky, "Efficient generation of 380fs pulses of THz radiation by ultrafast laser-pulse excitation of a biased semiconductor interface," *Appl. Phys. Lett.*, vol. 58, pp. 222–224, 1991.
[29] S. E. Ralph and D. Grischkowsky, "Trap-enhanced electric field effects in semi-insulators- the role of electrical and optical carrier injection," *Appl. Phys. Lett.*, vol. 59, pp. 1972–1974, 1991.
[30] Q. Wu, M. Litz, and X. C. Zhang, "Broadband and detection capability of ZnTe electro-optic field detectors," *Appl. Phys. Lett.*, vol. 68, pp. 2924–2926, 1996.
[31] X. C. Zhang, Y. Jin, K. Yang, and L. J. Scholwalter, "Resonant nonlinear susceptibility near the GaAs band gap," *Phys. Rev. Lett.*, vol. 69, pp. 2303–2306, 1992.
[32] M. van Exter, Ch. Fattinger, and D. Grischkowsky, "High brightness terahertz beams characterized with an ultrafast detector," *Appl. Phys. Lett.*, vol. 55, pp. 337–339, 1989.
[33] D. E. Aspnes and A. A. Studna, "Dielectric functions and optical parameters of Si, Ge, GeP, GaAs, GaSb, InP, InAs, and InSb from 1.5 to 6.0eV," *Phys. Rev. B*, vol. 27, pp. 985–1009, 1983.
[34] K. Wynne, private communication, May 1997.
[35] P. N. Saeta, J. F. Federici, B. I. Greene, and D. R. Dykaar, "Intervalley scattering in GaAs and InP probed by pulsed far-infrared transmission spectroscopy," *Appl. Phys. Lett.*, vol. 60, pp. 1477–1479, 1992.
[36] M. A. Osman, H. L. Grubin, P. Lugli, M. J. Kann, and D. K. Ferry, "Monte Carlo investigation of hot photo-excited electron relaxation in GaAs," in *Picosecond Electronics and Optoelectronics II*, F. J. Leonberger, C. H. Lee, F. Capasso, and H. Morkoc, Eds. Berlin, Germany: Springer-Verlag, 1987, p. 82–85.
[37] C. Kittel, *Introduction to Solid State Physics*, 7th ed. New York: Wiley, 1996.

Bret N. Flanders was born in Whittier, CA, on April 4, 1971. He received thr B.S. degree in chemical physics in 1993 from the University of California at San Diego, La Jolla, CA. From 1993 to 1997 he was a graduate student at the University of Pennsylvania. In 1997, he moved with Prof, N, F. Scherer to the University of Chicago, Chicago, IL, where he is currently working toward the Ph.D. degree in chemistry.

His research interests lie in the area of chemical reaction dynamics in the liquid phase, and particularly, on the experimental elucidation of reaction-induced solvent reorganization.

David C. Arnett was born in York, PA, on October 23, 1970. He received the B.S. degree in chemistry from Eastern College, St. Davids, PA, in 1992.

Since 1992, he has been a graduate research associate at the University of Pennsylvania, Philadelphia, PA, under the advisorship of Prof. N. F. Scherer. His research interests include the generation of femtosecond optical pulses and time resolved spectoscopic studies of chemical and biologically significant processes.

Norbert F. Scherer was born in Milwaukee, WI on July 9, 1960. He received the B.S. degree in chemistry from the University of Chicago, Chicago, IL, in 1982 and the Ph.D. degree in chemical physics from the California Institute of Technology, Pasadena, in 1989, working with Prof. A. Zewail.

He continued to work in the area of ultrafast laser spectroscopy as an NSF Post-Doctoral Fellow at the University of Chicago with Prof. G. Fleming. In 1992, he became an Assistant Professor of Chemistry at the University of Pennsylvania, Philadelphia. In 1997, he moved to the University of Chicago as Professor of Chemistry. His research interests include time-resolved nonlinear optical studies of chemical processes and reaction dynamics in condensed media, biological systems and at interfaces, development and application of nonlinear optical spectroscopies for further elucidation of molecular and material chromophore-bath interactions, scanning probe microscopy and the simultaneous correlation of structure with dynamics and reactivity through combined STM and femtosecond spectroscopy methods.

Dr. Scherer has received the American Chemical Society Proctor & Gamble Award for outstanding graduate research, and has been an Arnold and Mabel Beckman Foundation Young Investigator. He is currently an Alfred P. Sloan Research Fellow, a David And Lucile Packard Foundation Fellow, and a National Science Foundation National Young Investigator. He has also received a Camille Dreyfus Teacher-Scholar Award. He is a member of the American Chemical Society, America Physical Society, Optical Society of America, the Biophysical Society and the AAAS.